

1 **Numerical study of transport pathways of <sup>137</sup>Cs from forests to freshwater fish living in**  
2 **mountain streams in Fukushima, Japan**

3

4 Hiroshi Kurikami<sup>1\*</sup>, Kazuyuki Sakuma<sup>2</sup>, Alex Malins<sup>3</sup>, Yoshito Sasaki<sup>4</sup>, Tadafumi Niizato<sup>5</sup>

5 \*Corresponding author

6

7 <sup>1</sup>Japan Atomic Energy Agency (JAEA), Sector of Fukushima Research and Development,  
8 10-2 Fukasaku, Miharu-machi, Tamura-gun, Fukushima 963-7700, Japan,  
9 kurikami.hiroshi@jaea.go.jp, Tel: +81-247-61-2910

10

11 <sup>2</sup>Japan Atomic Energy Agency (JAEA), Sector of Fukushima Research and Development,  
12 10-2 Fukasaku, Miharu-machi, Tamura-gun, Fukushima 963-7700, Japan,  
13 sakuma.kazuyuki@jaea.go.jp

14

15 <sup>3</sup>Japan Atomic Energy Agency (JAEA), Center for Computational Science & e-Systems,  
16 University of Tokyo Kashiwanoha Campus Satellite, 178-4-4 Wakashiba, Kashiwa, Chiba  
17 277-0871, Japan, malins.alex@jaea.go.jp

18

19 <sup>4</sup>Japan Atomic Energy Agency (JAEA), Sector of Fukushima Research and Development,  
20 10-2 Fukasaku, Miharu-machi, Tamura-gun, Fukushima 963-7700, Japan,  
21 sasaki.yoshito@jaea.go.jp

22

23 <sup>5</sup>Japan Atomic Energy Agency (JAEA), Sector of Fukushima Research and Development,  
24 10-2 Fukasaku, Miharu-machi, Tamura-gun, Fukushima 963-7700, Japan,  
25 niizato.tadafumi@jaea.go.jp

26 Highlights

- 27 ● Cs-137 concentrations in some freshwater fish in Fukushima remain high, so a model  
28 was developed to assess uptake pathways.
- 29 ● Model assumed three export pathways from forests which supply soluble  $^{137}\text{Cs}$  to  
30 rivers were relevant for uptake by fish.
- 31 ● Pathways were direct litter fall into rivers, lateral inflow from litter, and transfer from  
32 soil via runoff and groundwater.
- 33 ● Data on  $^{137}\text{Cs}$  in forests, river water and freshwater fish measured across Fukushima  
34 were used for model calibration.
- 35 ● Fish  $^{137}\text{Cs}$  concentrations predicted to reach steady state after around 10 y due to  
36 equilibration of  $^{137}\text{Cs}$  cycle in forests.

37 **Abstract**

38       The accident at the Fukushima Dai-ichi Nuclear Power Plant in 2011 released a large  
39 quantity of radiocesium into the surrounding environment. Radiocesium concentrations in  
40 some freshwater fish caught in rivers in Fukushima Prefecture in October 2018 were still  
41 higher than the Japanese limit of 100 Bq kg<sup>-1</sup> for general foodstuffs. To assess the uptake of  
42 <sup>137</sup>Cs by freshwater fish living in mountain streams in Fukushima Prefecture, we developed a  
43 compartment model for the migration of <sup>137</sup>Cs on the catchment scale from forests to river  
44 water. We modelled a generic forest catchment with Fukushima-like parameters to ascertain  
45 the importance of three export pathways of <sup>137</sup>Cs from forests to river water for the uptake of  
46 <sup>137</sup>Cs by freshwater fish. The pathways were direct litter fall into rivers, lateral inflow from  
47 the forest litter layer, and lateral transfer from the underlying forest soil. Simulation cases  
48 modelling only a single export pathway did not reproduce the actual trend of <sup>137</sup>Cs  
49 concentrations in river water and freshwater fish in Fukushima Prefecture. Simulations  
50 allowing a combined effect of the three pathways reproduced the trends well. In the latter  
51 simulations, the decreasing trend of <sup>137</sup>Cs in river water and freshwater fish was due to a  
52 combination of the decreasing trend in the forest leaves/needles and litter compartments, and  
53 the increasing trend in soil. The modelled <sup>137</sup>Cs concentrations within the forest compartments  
54 were predicted to reach an equilibrium state at around ten years after the fallout due to the  
55 equilibration of <sup>137</sup>Cs cycling in forests. The model suggests that long term <sup>137</sup>Cs  
56 concentrations in freshwater fish in mountain streams will be controlled by the transfer of  
57 <sup>137</sup>Cs to river water from forest organic soils.

58

## 59 1. Introduction

60 The accident at the Fukushima Dai-ichi Nuclear Power Plant (FDNPP) in 2011 released  
61 a large quantity of radionuclides into the environment (Saito and Onda, 2015). Cesium-134  
62 and  $^{137}\text{Cs}$ , with half-lives of 2.1 and 30 years respectively, remain as the main radionuclides  
63 within the environment (Evrard et al., 2015). In the first few years following the accident,  
64 radiocesium concentrations in most agricultural and marine fish products dropped quickly  
65 (Wada et al., 2016b; Tagami and Uchida, 2016). However, as of October 2018, radiocesium  
66 concentrations in some freshwater fish caught within Fukushima Prefecture remain higher  
67 than the Japanese limit of  $100 \text{ Bq kg}^{-1}$  for general foodstuffs (Wada et al., 2016a, 2019;  
68 Ministry of Agriculture, Forestry and Fisheries, 2018a; Fukushima Prefecture, 2018ab). Fish  
69 caught both inside and outside the evacuation zone surrounding the FDNPP have exceeded  
70 this limit (Table 1). Examples include ayu (*Plecoglossus altivelis*), caught with up to about 2  
71  $\text{kBq kg}^{-1}$   $^{137}\text{Cs}$  in rivers near the FDNPP in 2016, masu salmon (*Oncorhynchus masou*)  
72 (resident form), e.g.  $126 \text{ Bq kg}^{-1}$   $^{137}\text{Cs}$  in a sample caught in a tributary of the Abukuma river  
73 in April 2018, and white-spotted char (*Salvelinus leucomaenis*),  $195 \text{ Bq kg}^{-1}$   $^{137}\text{Cs}$  in a sample  
74 caught in a tributary of the Abukuma river in October, 2018.

75 Freshwater fish caught in lakes and rivers traditionally make up a significant part of the  
76 Japanese diet. It is important therefore to understand the mechanisms of radiocesium export  
77 from overland to rivers which influence radiocesium concentrations in freshwater fish. It is  
78 thought that radiocesium exported from forests into the aquatic environment is the main  
79 source of radiocesium taken up by some species of freshwater fish living in mountain streams  
80 in Fukushima Prefecture (e.g. Murakami et al., 2014), as forests cover a major part of the  
81 contaminated catchments (c.a. 64% by area, Yamaguchi et al., 2014).

82 The main mechanism of export of radiocesium from forests to rivers is overland erosion  
83 and discharge of radiocesium-bearing soil particles into watercourses, essentially during

84 heavy rainfall events (Ueda et al., 2013; Nagao et al., 2013; Yamashiki et al., 2014). Around  
85 0.05 – 0.19% of the radiocesium inventory of Fukushima river catchments discharges into  
86 rivers annually due to soil erosion (Niizato et al., 2016). This mechanism is not however  
87 considered to be the main source of the radiocesium taken up by freshwater fish, as this  
88 radiocesium is strongly absorbed to soil particles and barely desorbs on the timescale of  
89 rainfall events (Murota et al., 2016; Mukai et al., 2018).

90 Dissolved radiocesium in river water is the most relevant fraction for biological  
91 availability (International Atomic Energy Agency, 2010). The dissolved fraction comprises  
92 around 12 – 91% of all radiocesium discharged through rivers under base flow conditions  
93 (Ochiai et al., 2015; Eyrolle-Boyer et al., 2016; Tsuji et al., 2016). It has been suggested that  
94 degradation of organic matter in forest litter could provide a source of dissolvable  
95 radiocesium for input into rivers (Sakuma et al., 2018). Submerged litter in rivers is  
96 considered to be another source of dissolvable  $^{137}\text{Cs}$  in aquatic ecosystems (Sakai et al., 2015;  
97 2016ab). In the field of nutrient cycling in freshwater ecosystems, previous studies have  
98 proved that direct litter fall and litter carried by surface runoff contributes to organic matter  
99 input into rivers (e.g. Kochi et al., 2010; Tonin et al., 2017). Thus the literature on inflows of  
100 radiocesium and other materials into rivers implies that there should be several radiocesium  
101 transport pathways from forests to rivers.

102 The objective of this study was to examine the  $^{137}\text{Cs}$  transport pathways from forests that  
103 affect  $^{137}\text{Cs}$  concentrations in freshwater fish living in mountain streams in Fukushima  
104 Prefecture. A compartment model was developed that simulates dissolved  $^{137}\text{Cs}$  circulation on  
105 the catchment scale between forests, rivers and freshwater fish. It was assumed for the model  
106 that only three transport pathways from forests leading to the input of dissolved  $^{137}\text{Cs}$  into  
107 river water were relevant for uptake by freshwater fish. The pathways were direct litter fall  
108 into rivers, lateral inflow from litter layers in forests, and lateral inflow from underlying forest

109 soils. The pathways encompass the input of litter, and the input of dissolved  $^{137}\text{Cs}$  produced  
110 by leaching from organic matter and desorption from soil minerals via surface runoff and  
111 groundwater flows.

112 We applied the model to a generic Fukushima-type forest catchment to evaluate the  
113 relative importance of the three transport pathways from forests for  $^{137}\text{Cs}$  uptake by  
114 freshwater fish. Datasets on  $^{137}\text{Cs}$  cycling in several forests in Fukushima Prefecture were  
115 used for model calibration and validation. Measurements for  $^{137}\text{Cs}$  concentrations in river  
116 water and freshwater fish from the Abukuma River and other coastal catchments in  
117 Fukushima Prefecture were used for discussion purposes and to provide comparisons for the  
118 simulation results. Note only  $^{137}\text{Cs}$  was modelled as the transfer dynamics of  $^{134}\text{Cs}$  were  
119 assumed to be identical.

120

## 121 2. Methods

### 122 2.1 Compartment model

123 A new compartment model was developed for this study to assess, on the river catchment  
124 scale,  $^{137}\text{Cs}$  transfer between leaves/needles, branches, bark, sap wood, heart wood, litter layer  
125 and soil in forests, discharge into rivers, and uptake by freshwater fish. For each compartment  
126  $i$ , the generic mass balance equation for  $^{137}\text{Cs}$  inventory  $A_i$  (Bq) is

127

$$128 \quad \frac{dA_i}{dt} = - \left\{ \lambda_p + \sum_{j=1, i \neq j}^n \lambda_{ij} \right\} A_i + \sum_{j=1, i \neq j}^n \lambda_{ji} A_j \quad (1)$$

129

130 where  $t$  is time (yr),  $\lambda_p$  is the physical decay constant of  $^{137}\text{Cs}$  ( $\text{yr}^{-1}$ ) and  $\lambda_{ij}$  is the transfer rate  
131 from compartment  $i$  to compartment  $j$  ( $\text{yr}^{-1}$ ).

132 Figure 1 shows a schematic of the compartments in the model. Each forest type

133 comprised seven compartments: leaves/needles, branches, bark, sap wood, heart wood, litter  
134 layer and soil. The cycling of radiocesium in forests in Fukushima Prefecture broadly depends  
135 on whether the stand is deciduous or coniferous (Imamura et al., 2017). Deciduous and  
136 coniferous forests were therefore represented as separate entities in the model, i.e. each type  
137 was given its own group of seven forest compartments (Fig. 2).

138 A river compartment was linked to the leaves/needles, litter layer and soil compartments  
139 in both deciduous and coniferous forests. These links model implicitly the following physical  
140 processes. The link from the leaves/needles compartment models litter fall directly into rivers  
141 and its subsequent breakdown which leaches  $^{137}\text{Cs}$  into river water. The link from the litter  
142 layer models litter transferred by surface runoff into rivers and its subsequent breakdown, and  
143 also leaching from litter on the forest floor which inputs dissolved  $^{137}\text{Cs}$  into surface runoff  
144 and groundwater flows, and on into rivers. The link from the soil compartment models  $^{137}\text{Cs}$   
145 leaching from underlying forest soils into surface water and groundwater and subsequent flow  
146 into rivers. Note submerged litter was not modelled as a separate compartment, as  $^{137}\text{Cs}$   
147 leaching from submerged litter was considered to occur on a timescale faster than that  
148 relevant for the compartment model. This was based on experiments showing  $^{137}\text{Cs}$  leaching  
149 from submerged litter occurs over the timescale of a few days (Sakai et al., 2015).

150 A downstream compartment was connected to the river compartment and used as a sink  
151 for the model catchment. Thus in total there were sixteen main compartments in the model.  
152 An interaction matrix for the compartments is shown in Fig. 2. The compartments and  
153 processes in our model are similar to existing forest models (e.g., International Atomic Energy  
154 Agency, 2002; Nishina and Hayashi, 2015; Nishina et al., 2018; Thiry et al., 2018). The  
155 compartments were chosen to coincide with the main types of monitoring data available for  
156 Fukushima Prefecture from previous studies (Ministry of Agriculture, Forestry and Fisheries,  
157 2018b; Komatsu et al., 2016; Imamura et al., 2017).

158 A fish compartment was connected to the river compartment to model  $^{137}\text{Cs}$  uptake by  
 159 freshwater fish. As previous studies reported, freshwater fish take up  $^{137}\text{Cs}$  not from water but  
 160 mainly from food, and the apparent transfer factor, i.e. the ratio of  $^{137}\text{Cs}$  concentration in fish  
 161 to that in water, depends on the trophic level (e.g., Rowan et al., 1998; Tuovinen et al., 2012;  
 162 Sundbom et al., 2003). On the other hand, commonly used bioaccumulation models assume  
 163 that radionuclide concentrations in aquatic organisms are in equilibrium with a reference  
 164 medium in the surrounding environment such as water or sediment (International Atomic  
 165 Energy Agency, 2010). This assumption means models can be significantly simplified by not  
 166 having to model full details of the food chain. Moreover detailed food chain models are often  
 167 unjustified due to large uncertainties in the transfer parameters between food chain elements.  
 168 Figure 3 shows a strong relationship between  $^{137}\text{Cs}$  concentrations in water and in fish in  
 169 Fukushima, which justifies the idea that river water can be used as a reference medium.

170 In this study, the transfer model from river water to fish was identical for all species. The  
 171 model represented all the dynamic processes of food chains (uptake to fish via plankton,  
 172 worms etc.) implicitly by using the following pseudo first-order kinetic equation

173

$$\begin{aligned}
 & \frac{dc_{fish}}{dt} = k(Tc_{water} - c_{fish}) \\
 & k = \begin{cases} k_{up} & \text{when } Tc_{water} \geq c_{fish} \\ k_{ex} & \text{when } Tc_{water} < c_{fish} \end{cases}
 \end{aligned}
 \tag{2}$$

175

176 where  $c_{fish}$  and  $c_{water}$  are the  $^{137}\text{Cs}$  concentrations in fish ( $\text{Bq kg}^{-1}$ ) and water ( $\text{Bq m}^{-3}$ ),  
 177 respectively,  $T$  is the transfer factor in the equilibrium state ( $\text{m}^3 \text{kg}^{-1}$ ),  $k$  is the kinetic rate ( $\text{yr}^{-1}$ ).  
 178 Different kinetic rates were adopted for uptake,  $k_{up}$ , and excretion,  $k_{ex}$ .  $c_{water}$  was obtained by  
 179 dividing the total  $^{137}\text{Cs}$  inventory in river water by the total river water volume. It was  
 180 assumed that  $^{137}\text{Cs}$  uptake by fish did not alter the mass balance in the rest of the system.

181

## 182 2.2 Modelling of generic Fukushima-type forest catchment

183 In this study we modelled a generic river catchment by using parameters with general  
184 applicability for contaminated forest catchments in Fukushima Prefecture. The model  
185 included only forest and river land uses, i.e. no urban, paddy or grass areas were included.  
186 The ratio of deciduous to coniferous forest by area was assumed to be 4 to 1, in accordance  
187 with the average for Fukushima Prefecture measured from a land use map (Japan Aerospace  
188 Exploration Agency, 2018). The ratio of river to the forest area was assumed to be 0.01, based  
189 on the land use map. In order to calculate the total river water volume, a mean river water  
190 depth of 0.4 m was assumed, based on field measurements of rivers such as the Ukedo River  
191 in Fukushima Prefecture (Onishi et al., 2014). The annual precipitation was assumed to be  
192 1200 mm yr<sup>-1</sup> and the ratio of runoff to precipitation was 0.6, based on the average for  
193 Fukushima Prefecture (Japan Meteorological Agency, 2018; Unoki, 2010).

194 Inventories of <sup>137</sup>Cs in each compartment were normalized by the total inventory per unit  
195 area of the catchment for all calculations. Thus, the results are independent of total <sup>137</sup>Cs  
196 inventory of the catchment. The model assumes a homogeneous <sup>137</sup>Cs distribution over the  
197 catchment, i.e. constant <sup>137</sup>Cs radioactivity per area. The normalization means the results are  
198 also independent of the catchment size.

199

## 200 2.3 Setting of transfer parameters and initial state of model

201 The main parameters in the model are the transfer rates  $\lambda_{ij}$  between the compartments,  
202 the <sup>137</sup>Cs transfer factor between fish and river water  $T$ , and its associated rate constant  $k$ . The  
203 initial state of the model was the relative radioactivity of each compartment on March 15,  
204 2011. The following sections describe the way the parameters and the initial state of the  
205 model were set. In brief, the transfer rates between forest compartments were obtained by

206 fitting monitored  $^{137}\text{Cs}$  concentrations within four forests in Fukushima Prefecture between  
207 2011-2017. Transfer rates for the forest to river water pathways (direct litter fall, lateral inflow  
208 from litter and from soil) were investigated by numerical exploration of the parameter space.  
209 Transfer parameters for  $^{137}\text{Cs}$  uptake by freshwater fish were assigned based on measured  
210  $^{137}\text{Cs}$  concentrations of freshwater fish and river water. The transfer rate from rivers to the  
211 downstream compartment was fixed to ensure the overall mass balance of water in the  
212 system.

213

### 214 2.3.1 Inverse analysis to estimate fallout interception ratios and transfer rates in forests

215 The initial  $^{137}\text{Cs}$  inventories and transfer rates for forest compartments were estimated  
216 by fitting monitoring results from one deciduous forest (konara oak, *Quercus serrata*) in  
217 Otama village (OT-Q), and three coniferous forests in Kawauchi village in Fukushima  
218 (Ministry of Agriculture, Forestry and Fisheries, 2018b). The Kawauchi coniferous forests  
219 were the hinoki cypress (*Chamaecyparis obtusa*) forest, KU1-H, and Japanese cedar  
220 (*Cryptomeria japonica*) forests, KU1-S and KU2-S (Imamura et al, 2017). As the goal of the  
221 study was to examine the  $^{137}\text{Cs}$  transport pathways from forests affecting the  $^{137}\text{Cs}$   
222 concentration of freshwater fish, it was considered reasonable to use a backwards fitting  
223 approach to obtain the transfer parameters pertinent to internal cycling in the forests. An  
224 approach based on direct measurements of the transfer rates was not considered feasible.

225 The atmospheric fallout at March 15, 2011 was assumed to be the sole input of  $^{137}\text{Cs}$   
226 to the system. No inventory was applied to sap wood, heart wood and soil beneath the litter  
227 layer in the initial state. The relative interception of the  $^{137}\text{Cs}$  fallout by the leaf/needle, branch,  
228 bark and litter compartments and the transfer rates between the forest compartments were  
229 obtained by minimizing the objective function

230

231 
$$f = \sum_i w_i (\log y_{sim,i} - \log y_{meas,i})^2 . \quad (3)$$

232

233 Here  $y_{sim,i}$  and  $y_{meas,i}$  are respectively the simulated and measured relative  $^{137}\text{Cs}$  concentrations  
234 in compartment  $i$  at time  $t$  ( $i = \text{leaves/needles, branch, bark, sap wood, heart wood, litter layer}$   
235 and soil), and  $w_i$  are weights that were chosen manually as to obtain reasonable fitting results.

236 The objective function was minimized using an iterative process whereby a  $\pm 4\%$   
237 alteration was made to one parameter at a time. If the change resulted in  $f$  decreasing, the  
238 changed parameter was accepted. The iterative process of testing trial changes to the  
239 parameters continued until no further changes were acceptable and the process had converged.  
240 During this fitting process, the outward flux of  $^{137}\text{Cs}$  from forests was neglected.

241 The initial interception ratios and forest compartment transfer rates estimated by the  
242 inverse fitting analysis were cross-checked against an independent set of results from Kato et  
243 al. (2017, 2018b). The Kato et al. results are initial interception ratios and radiocesium  
244 transfer fluxes from the tree canopy to the forest floor in a mixed-broadleaf forest, mature  
245 cedar forest, and a young cedar forest in Kawamata town in Fukushima.

246

### 247 2.3.2 Numerical exploration of transfer parameters from forests to rivers

248 No appropriate measurements were available for the relative importance of the three  
249 transfer pathways in the model from forests to rivers. Thus we investigated the transfer  
250 parameters for these pathways numerically by exploring the parameter space with various  
251 simulation cases (Table 2). It was assumed that the transfer rates for the three compartments  
252 connected to rivers were constants.

253 In the first three cases (Case 1 to 3) a single transport pathway was assumed: Case 1 –  
254 only lateral inflow from soil; Case 2 – only lateral inflow from the litter layer; and Case 3 –  
255 only direct litter fall into rivers. The transfer rate for each case was estimated from the bulk

256 transfer rate from forests to rivers  $\lambda_{forest\_to\_river}$  ( $yr^{-1}$ ) at around two years after the fallout. The  
 257 bulk transfer rate at this time was obtained as the ratio of the annual  $^{137}Cs$  discharge via the  
 258 catchment outlet to the total  $^{137}Cs$  inventory in the catchment:

259

$$260 \quad \lambda_{forest\_to\_river} = \frac{c_{water} \times R}{I} . \quad (4)$$

$$R = P \times a \times r$$

261

262 Here  $R$  is the annual runoff ( $m^3 yr^{-1}$ ),  $I$  is the  $^{137}Cs$  total inventory in the catchment (Bq),  $P$  is  
 263 the annual precipitation  $P = 1.2$  ( $m yr^{-1}$ ),  $a$  is the catchment area ( $m^2$ ) and  $r$  is the ratio of  
 264 runoff to precipitation  $r = 0.6$  (dimensionless). The bulk transfer rate  $\lambda_{forest\_to\_river}$  changes over  
 265 time but can be estimated at certain time points. Yoshimura et al. (2015) showed that the  
 266 dissolved  $^{137}Cs$  concentration of river water ( $Bq m^{-3}$ ) was related to the average catchment  
 267 inventory ( $Bq m^{-2}$ ) at around two years after the deposition by

268

$$269 \quad c_{water} = 8.6 \times 10^{-5} \times \frac{I}{a} . \quad (5)$$

270

271 Thus we can derive

272

$$273 \quad \lambda_{forest\_to\_river} = 6.2 \times 10^{-5} yr^{-1} . \quad (6)$$

274

275 The ratios of  $^{137}Cs$  inventories in forest compartments for two years after the deposition  
 276 were roughly 60% in soil, 30% in litter layer and 0-5% in leaves/needles, thus we set the  
 277 transfer rate from soil to river in Case 1 as  $6.2 \times 10^{-5} / 0.645 \times 1.5 = 1.4 \times 10^{-4} yr^{-1}$ , the transfer  
 278 rate from litter layer to river in Case 2 as  $6.2 \times 10^{-5} / 0.345 \times 1.5 = 2.7 \times 10^{-4} yr^{-1}$ , and the

279 transfer rate from leaves/needles to river in Case 3 as  $6.2 \times 10^{-5} / 0.01 \times 1.5 = 9.3 \times 10^{-3} \text{ yr}^{-1}$ ,  
280 respectively. Here, the values of 0.645, 0.345 and 0.01 were assumed instead of 0.6, 0.3 and  
281 0-0.05 so that the sum total is 1.0.

282 The value of 1.5 was added as a tuning parameter. Tuning was necessary because the  
283  $^{137}\text{Cs}$  concentrations in river water measured by Yoshimura et al. (2015) were about 1.5 times  
284 smaller than the more comprehensive measurements from the Ministry of Environment  
285 (2018) used to validate the compartment model. Since this study focuses on the time trend of  
286  $^{137}\text{Cs}$  in water and fish rather than the absolute values of  $^{137}\text{Cs}$  concentrations, and the value  
287 of 1.5 itself is not significant considering the uncertainties in the other parameters, this tuning  
288 step is not considered to affect the conclusions of this study.

289 Cases 4-6 allowed multiple pathways for  $^{137}\text{Cs}$  export from forests to river (Table 2).  
290 Case 4 permitted transfers from the leaf/needle and litter layer compartments to river water.  
291 The transfer parameters used meant each transfer pathway contributed 50% of the total  
292 discharge flux from forests to rivers at the two year time point (i.e. on March 15, 2013). No  
293 flux from the soil was allowed in Case 4. Cases 5 and 6 allowed contributions from all three  
294 pathways. The transfer parameters chosen for Case 5 meant that the soil to river water  
295 pathway constituted 10% of the total forest to river flux, and the litter fall and litter layer  
296 pathways contributed in equal amounts (i.e. 45% each), at the two year time point. The  
297 parameters chosen for Case 6 meant the soil to river pathway contributed 50% of the total flux,  
298 and the other pathways 25% each, at the two year point.

299

### 300 2.3.3 Other transfer parameters

301 The transfer rate from the river compartment to downstream compartment  
302  $\lambda_{\text{river\_to\_downstream}}$  was

303

$$\lambda_{river\_to\_downstream} = \frac{R}{V_{river}} \quad (7)$$

$$V_{river} = a \times 0.01 \times 0.4$$

305

306 where  $V_{river}$  is the total river water volume ( $m^3$ ). Thus  $\lambda_{river\_to\_downstream}$  yields

307

$$\lambda_{river\_to\_downstream} = 1.8 \times 10^2 \text{ yr}^{-1}.$$

309

310 Eq. (7) ensures the mass balance of the system.

311 The transfer factor from river water ( $Bq \text{ m}^{-3}$ ) to freshwater fish ( $Bq \text{ kg}^{-1}$ ) was assumed to  
 312 be  $1.6 \text{ m}^3 \text{ kg}^{-1}$  based on measured  $^{137}\text{Cs}$  concentrations in freshwater fish and dissolved  $^{137}\text{Cs}$   
 313 concentrations in river water (data from Ministry of Environment, 2018 and Japan Atomic  
 314 Energy Agency, 2018). The plots in Fig. 3 include data for two different feeding types of fish,  
 315 masu salmon *Oncorhynchus masou* (resident form), a carnivorous fish, and Japanese dace  
 316 *Tribolodon hakonensis*, an omnivorous fish. Although previous studies (e.g. Nasvit et al.,  
 317 2007; Wada et al., 2016a) noted  $^{137}\text{Cs}$  concentrations varied between species, there is no  
 318 obvious difference between two species in the data in Fig. 3. The kinetic rate for transfer from  
 319 river water to freshwater fish was set based on results from experiments by Fukushima  
 320 Prefecture (2018c). The Prefecture released uncontaminated fish (masu salmon in resident  
 321 form) into rivers, and collected them after two days to two months, to measure their  $^{137}\text{Cs}$   
 322 concentrations. The results indicated a kinetic rate  $k_{up}$  of 2.2 - 4.5  $\text{yr}^{-1}$ . In the simulations,  
 323 3.4  $\text{yr}^{-1}$  was adopted which is the middle of this range. The kinetic rate of  $^{137}\text{Cs}$  excretion  $k_{ex}$   
 324 was assumed to be 2.5  $\text{yr}^{-1}$ , which corresponds to a 100 day biological half-life.

325

### 326 3. Results and discussions

#### 327 3.1 Fitting initial interception ratios and the transfer rates within forests

328 Figure 4 shows the measurement and compartment model results for the partitioning of  
329  $^{137}\text{Cs}$  within forests over a 10 year period from March 15, 2011. The results for each  
330 compartment are shown relative to the total forest  $^{137}\text{Cs}$  inventory. The compartment model  
331 data apply after convergence of the fitting process for the initial inventories of the leaf/needle,  
332 branch, bark and litter layer compartments and the transfer rates ( $\lambda_{ij}$ ) between the forest  
333 compartments.

334 The weights  $w_i$  in the objective function (Eq. (3)) were all set as 1 when fitting the  
335 measurements for the coniferous forests in Kawauchi (Fig. 4(b) to (d)). For the deciduous  
336 forest in Otama (OT-Q, Fig. 4(a)), it was necessary to increase the weights  $w_i$  for the leaf,  
337 litter and soil compartments to 5. This change was made so that the simulations produced  
338 good matches with the measurements for  $^{137}\text{Cs}$  concentrations in compartments linked to  
339 rivers (cf. Fig. 4(a) and Fig. S1(a), the latter of which shows results with  $w_i$  all equal to 1).  
340 Note for the Kawauchi forests, acceptable matches were obtained irrespective of whether  
341 these weights were 1 or 5 (cf. Fig. 4(b) to (d) and Fig. S1(b) to (d)). Tables 3 and 4 summarize  
342 the initial interception ratios and the transfer rates obtained from the parameter fitting process  
343 (as per results in Fig. 4).

344 Similar trends of the relative  $^{137}\text{Cs}$  concentrations in forest compartments could be seen  
345 for all forest sites in Fig. 4. The  $^{137}\text{Cs}$  concentrations in leaves/needles, branches, bark and the  
346 litter layer decreased with time, while those in sap wood, heart wood and soil increased to a  
347 plateau. At long times the majority of  $^{137}\text{Cs}$  within the forests was located within the soil.

348 Measurements from deciduous forests were only available for the konara oak site in  
349 Otama village (OT-Q). Thus the transfer rates for OT-Q were adopted as the parameter set for  
350 deciduous forests in the hereafter compartment model simulations. Although a slight  
351 difference between the simulations and measurements could be seen for the  $^{137}\text{Cs}$   
352 concentration in branches for site OT-Q (Fig. 4(a)), this compartment was not connected

353 directly to river water thus this difference did not have a significant effect on the following  
354 discussions. The plateauing of the results at ~10 years was indicative of equilibrium being  
355 reached for internal cycling of the  $^{137}\text{Cs}$  within forests.

356 The internal transfer parameters for coniferous forests were established separately for the  
357 three sites where measurement data were available: the hinoki cypress forest (KU1-H) and the  
358 Japanese cedar forest plots (KU1-S and KU2-S) in Kawauchi village. The transfer parameters  
359 obtained for KU1-S (Fig. 4(c)) were adopted as the reference for coniferous forests in the  
360 following simulations, as measurement data were available for within the first year after the  
361 fallout for this site only.

362 We cross checked the initial interception ratios and the transfer rates estimated by the  
363 parameter fitting process with independent measurements from Kato et al. (2017, 2018b).  
364 Kato et al. (2017) reported that the canopy interception ratios for a mixed forest, a mature  
365 cedar forest, and a young cedar forest of 0.23, 0.69 and 0.70, respectively. As shown in Table  
366 3, the interception ratio for the Otama deciduous forest was 0.32, while the results for the  
367 Kawauchi coniferous forests were 0.31-0.55. The results suggest that coniferous forests had  
368 higher interception ratios than deciduous forests. This is explained by deciduous trees being  
369 leafless at the time of the fallout in March 2011. Considering the heterogeneity of the  $^{137}\text{Cs}$   
370 distribution in forest (e.g., Kato et al., 2018a; Takada et al., 2016; Imamura et al., 2018), and  
371 the uncertainty in the measurements at the different sites, the interception ratios derived by the  
372 inverse analysis were in reasonably good agreement with the measurements.

373 Most transfer rates such as root uptake and translocation inside trees cannot be measured  
374 directly. Therefore we only compared internal  $^{137}\text{Cs}$  fluxes within forests against  
375 measurements of Kato et al. (2018b) of through fall (TF), litter fall (LF) and stem flow (SF)  
376 rates (Fig. 5). The measured  $^{137}\text{Cs}$  fluxes ( $\text{Bq m}^{-2} \text{ yr}^{-1}$ ) were normalized by dividing by the  
377 deposition inventories for each site ( $\text{Bq m}^{-2}$ ). The combined TF and LF fluxes correspond to

378 the transfer from leaves/needles and branches to the litter layer in the compartment model.  
379 The SF flux corresponds to the transfer from bark to the litter layer in the compartment  
380 model.

381 The graphs in Fig. 5 show large fluctuations between measurement points. The simulated  
382  $^{137}\text{Cs}$  fluxes were generally consistent with the order of magnitude of the measurements,  
383 hence justifying the transfer rates obtained by the inverse fitting analysis. The estimated  
384 transfer rates from leaves/needles to the litter layer shown in Table 4, specifically 0.52-1.3  $\text{yr}^{-1}$   
385 for coniferous forests and 2.59  $\text{yr}^{-1}$  for deciduous forests, were comparable with the range of  
386 0.15-1.5  $\text{yr}^{-1}$  for coniferous forests and 0.14-4.3  $\text{yr}^{-1}$  for deciduous forests estimated by  
387 Hashimoto et al. (2013). The transfer rates from the litter layer to soil, 0.20-0.67  $\text{yr}^{-1}$  for  
388 coniferous forests and 0.59  $\text{yr}^{-1}$  for deciduous forests, were in an agreement with the  
389 Hashimoto et al. (2013) estimates, which were 0.34-6.8  $\text{yr}^{-1}$  and 0.34-5.8  $\text{yr}^{-1}$  respectively.

390

### 391 3.2 Transfer processes of $^{137}\text{Cs}$ from forests to freshwater fish

392 After confirming the applicability of the forest parameters obtained by the inverse fitting  
393 process, we proceeded to evaluate feasible transfer parameters for  $^{137}\text{Cs}$  export from forests to  
394 rivers by numerical exploration of the parameter space. Figure 6 shows the results of Case 1  
395 to 3 simulations and measurements for the relative  $^{137}\text{Cs}$  concentrations in river water  
396 (dissolved) and in freshwater fish (Ministry of Environment, 2018; Japan Fisheries Research  
397 and Education Agency, 2017). The measurement samples were collected from the Abukuma  
398 River, which flows from south to north through central Fukushima Prefecture, its tributaries,  
399 and several rivers in the coastal area of the Prefecture. Measured concentrations of  $^{137}\text{Cs}$   
400 dissolved in river water and in fish were normalized by the mean inventory of the area  
401 upstream of the locations where samples were taken (using data from the second airborne  
402 survey, Nuclear Regulation Authority, 2018; data downloaded from Japan Atomic Energy

403 Agency, 2018). In Case 1, the relative concentrations of  $^{137}\text{Cs}$  dissolved in river water and  
404 within fish increased over time. This is because as  $^{137}\text{Cs}$  migrated over time into the forest soil  
405 layer, this  $^{137}\text{Cs}$  became available in the model for export to rivers. The results of Case 1 were  
406 not consistent with the measurements, which show a gradual decrease of the relative  $^{137}\text{Cs}$   
407 concentrations over time. Therefore  $^{137}\text{Cs}$  export from forests due to litter fall into rivers and  
408 lateral inflows from the litter layer could not be ignored.

409 Cases 2 and 3, where only litter layer or litter fall to river fluxes were allowed  
410 respectively, showed decreasing relative  $^{137}\text{Cs}$  concentrations over time. The rates of decrease  
411 were slightly higher than that for the measurements, however. Collectively these results  
412 demonstrate that a single pathway cannot explain the measured trend of  $^{137}\text{Cs}$  concentrations  
413 in freshwater fish.

414 The results of the simulation cases allowing multiple export pathways are shown in Fig.  
415 7. Case 4 allowed both the litter fall and litter layer transfers to river water. Comparing with  
416 Cases 2 and 3, Case 4 yielded results closer to the monitoring data (cf. Fig. 7(a) and (b) with  
417 Fig. 6(a) and (b)) for the initial two year period. However for later years Case 4  
418 underestimated the relative  $^{137}\text{Cs}$  concentrations. This result suggests that the soil to river  
419 water transfer pathway cannot be ignored. This is reasonable as, in later years, the majority of  
420  $^{137}\text{Cs}$  within forests is located within soil. Therefore soil to river transfer is likely to be an  
421 important contributor of  $^{137}\text{Cs}$  input to river water in later years.

422 In Cases 5 and 6, the transfer pathways from forest soil to river water were switched on.  
423 In Case 5, 10% of the total dissolved  $^{137}\text{Cs}$  input to river water at the two year time point was  
424 attributable to discharge from the soil layer. The results of Case 5 were closest to the  
425 measurements (Fig. 7). Case 6 tended to overestimate the monitored  $^{137}\text{Cs}$  concentrations for  
426 later years. This suggests the transfer rate from soil to river water was too large in Case 6. The  
427 above results suggest that the trend of  $^{137}\text{Cs}$  concentrations dissolved in river water and within

428 fish is attributable the changes in concentration levels in leaves, needles, the litter layer and  
429 soil in forests over time.

430 Figure 8 shows the components of the  $^{137}\text{Cs}$  fluxes into river water calculated from Case  
431 5. During the first two years, this model indicated the transfer from leaves and needles (direct  
432 litter fall) followed by transfer from the litter layer were the dominant processes. There was a  
433 cross-over at two years, upon which transfer from the litter layer became most significant  
434 until the 4.5 year time point. After 4.5 years, flux from soil became the most important export  
435 pathway to river water. The contributions of the three pathways predicted in this model  
436 stabilized at around ten years as the  $^{137}\text{Cs}$  cycling within forests reaches equilibrium.

437 It has been reported that there are two or three different characteristic timescales for the  
438 decrease in  $^{137}\text{Cs}$  concentrations dissolved in river water and within freshwater fish (e.g.,  
439 Smith et al., 2002; Nakanishi and Sakuma, 2018). Analyses of fallout from atmospheric  
440 nuclear weapons testing and the Chernobyl accident suggest that the radiocesium removal rate  
441 from catchments is related to soil properties such as clay mineral and organic content (Smith  
442 et al., 2002; Spezzano et al., 1993), however these factors were not analyzed in this study. The  
443 assumptions and judgements taken in this study yielded a model where the different  
444 characteristic timescales are explained by the redistribution of  $^{137}\text{Cs}$  that occurs within forests,  
445 rather than differences in soil properties. In the initial stage after fallout, the fast rate of  
446 decrease of  $^{137}\text{Cs}$  concentrations in river water and fish was attributed to the fast decrease of  
447  $^{137}\text{Cs}$  concentrations in forest litter, leaves and needles. On the other hand, the long term  
448 slower rate of decrease is controlled by the export of  $^{137}\text{Cs}$  from forest soil in our  
449 compartment model. Since radiocesium is strongly fixed to mineral particles in soil, the  
450 organic component in soil is likely to be the most important component for dissolved  $^{137}\text{Cs}$   
451 export from the soil layer if our assumptions hold true.

452 The rate of export of  $^{137}\text{Cs}$  from forest soil will likely depend on the distribution of the

453  $^{137}\text{Cs}$  with depth and existing forms within the soil. These factors cannot be accounted in the  
454 current compartment model, unless modifications are made, as the soil to river water export  
455 rate was assumed to be constant. Previous measurements in Fukushima Prefecture (e.g.,  
456 Imamura et al., 2017; Nakanishi et al., 2014) have shown gradual migration of  $^{137}\text{Cs}$  deeper  
457 into forest soil over time, albeit with a slow rate. Studies of the Chernobyl accident and global  
458 nuclear weapons fallout (e.g., International Atomic Energy Agency, 2006; Koarashi et al.,  
459 2017) reported  $^{137}\text{Cs}$  remained mostly in the upper layers of forest soil. Further studies in  
460 Fukushima revealed that organic matter in forest soil played an important role in retaining  
461  $^{137}\text{Cs}$  (Koarashi et al., 2019; Koarashi and Atarashi-Andoh, 2019). According to our  
462 compartment model, affected species of freshwater fish in catchments with forests will  
463 continue to take up  $^{137}\text{Cs}$  over the long term. This is due to the continuous input of dissolved  
464  $^{137}\text{Cs}$  into river water over time from the forest soil layer in the model. However a firm  
465 conclusion cannot be drawn as the effects of  $^{137}\text{Cs}$  migration into soil and fixation to clay  
466 mineral need to be assessed with a more detailed model.

467 The measured  $^{137}\text{Cs}$  concentrations in two fish species with different feeding habits are  
468 within an order of magnitude of each other (Fig. 7(b)). This implies that the source of the  
469  $^{137}\text{Cs}$  within these fish is basically the same even if the food chains are different. However, the  
470 spread of the  $^{137}\text{Cs}$  concentrations measured within fish (Fig. 7(b)) is larger than that for  
471 dissolved  $^{137}\text{Cs}$  concentrations within river water (Fig. 7(a)). This may be due to the wide  
472 variety of sizes of individuals and supporting food chains for different species. Simulation  
473 Case 5 reproduced the trend of the measurements from six years of monitoring best (Fig. 7).  
474 Continued monitoring is needed for future years to check whether the curve predicted by Case  
475 5 is true, and to understand long-term freshwater fish  $^{137}\text{Cs}$  concentrations and uptake  
476 mechanisms.

477 This study focused on mountainous catchments covered by forests as these are typical

478 catchments in Fukushima Prefecture. However, the modeling concept used here, that  
479 considers the link between the overland  $^{137}\text{Cs}$  behavior and rivers, is expected to be useful for  
480 other types of catchment. This is because the chemical components in rivers are always  
481 affected by the overland environment.

482

#### 483 4. Conclusions

484 In this paper a compartment model was developed to assess catchment-scale migration of  
485  $^{137}\text{Cs}$  and evaluate three potential transport pathways of  $^{137}\text{Cs}$  from forests to fish living in  
486 mountain streams. Under the modelling assumptions used, the decreasing trend over time of  
487  $^{137}\text{Cs}$  concentrations dissolved in river water and within freshwater fish was explained by the  
488 decreasing trend of  $^{137}\text{Cs}$  concentrations in leaves/needles and litter layer and the increasing  
489 trend in organic soil. The fluxes predicted from the model reached equilibrium at around ten  
490 years after the initial fallout due to  $^{137}\text{Cs}$  circulation within forests reaching a steady state.  
491 Modelled reductions in  $^{137}\text{Cs}$  concentrations in river water and freshwater fish over the long  
492 term are then controlled by the rate of physical decay of  $^{137}\text{Cs}$ .

493 This paper focused only on species of freshwater fish living in mountain streams with  
494 short water residence times. In such an “open” system,  $^{137}\text{Cs}$  flux from forests controls the  
495 contamination levels of the fish. However, for fish in “closed” systems with long residence  
496 times, such as lakes, the internal circulation of  $^{137}\text{Cs}$  within the system is more complex, and  
497 transfers between water, bed sediment and levels of the food chain should be considered.  
498 Further field investigations and modelling improvements are required to understand the  
499 sources of  $^{137}\text{Cs}$  taken up by freshwater fish in closed systems.

500

#### 501 Acknowledgments

502 The authors would like to appreciate the reviewers for their precious comments and

503 suggestions on the manuscript. We thank members of the Fukushima Environmental Safety  
504 Center for their support for the study. We also appreciate M. Kanno and T. Sugita for their  
505 assistance with respect to the simulations.

506

507

508 References

- 509 Evrard, O., Laceby, J. P., Lepage, H., Onda, Y., Cerdan, O., Ayrault, S., 2015. Radiocesium  
510 transfer from hillslopes to the Pacific Ocean after the Fukushima Nuclear Power Plant  
511 accident: A review. *J. Environ. Radioact.* 148, 92–110. doi:  
512 10.1016/j.jenvrad.2015.06.018.
- 513 Eyrolle-Boyer, F., Boyer, P., Garcia-Sanchez, L., Métivier, J.M., Onda, Y., De Vismes, A.,  
514 Cagnat, X., Boulet, B., Cossonnet, C., 2016. Behaviour of radiocaesium in coastal rivers  
515 of the Fukushima Prefecture (Japan) during conditions of low flow and low turbidity -  
516 insight on the possible role of small particles and detrital organic compounds. *J. Environ.*  
517 *Radioact.* 151, 328–340. doi: 10.1016/j.jenvrad.2015.10.028.
- 518 Fukushima Prefecture, 2018a, Fukushima prefecture agriculture, forestry and fisheries  
519 products processed food monitoring information. (Accessed 18 December 2018) at  
520 <https://www.new-fukushima.jp/top>.
- 521 Fukushima Prefecture, 2018b, 平成 28 年度事業概要報告書 (FY2016 Summary Report (in  
522 Japanese). (Accessed 20 September 2018) at  
523 [https://www.pref.fukushima.lg.jp/uploaded/life/248127\\_710135\\_misc.pdf](https://www.pref.fukushima.lg.jp/uploaded/life/248127_710135_misc.pdf).
- 524 Fukushima Prefecture, 2018c, 異なる体サイズのヤマメ人工種苗における  $^{137}\text{Cs}$  蓄積  
525 (Accumulation of  $^{137}\text{Cs}$  to different sizes of masu salmon (resident form) by seedling  
526 experiments) (in Japanese). (Accessed 20 September 2018) at  
527 <https://www.pref.fukushima.lg.jp/uploaded/attachment/261601.pdf>.
- 528 Hashimoto, S., Matsuura, T., Nanko, K., Linkov, I., Show, G., Kaneko, S., 2013. Predicted  
529 spatio-temporal dynamics of radiocesium deposited onto forests following the  
530 Fukushima nuclear accident. *Sci. Rep.* 3, 2564. doi: 10.1038/srep02564.
- 531 Imamura, N., Komatsu, M., Ohashi, S., Hashimoto, S., Kajimoto, T., Kaneko, S., Takano, T.,  
532 2017. Temporal changes in the radiocesium distribution in forests over the five years

533 after the Fukushima Daiichi Nuclear Power Plant accident. *Sci. Rep.* 7, 8179.  
534 doi:10.1038/s41598-017-08261-x.

535 Imamura, N., Kobayashi, M., Kaneko, S., 2018. Forest edge effect in a radioactivity  
536 contaminated forest in Fukushima, Japan. *J. Forest Res.* 23, 15-20. doi:  
537 10.1080/13416979.2017.1396417.

538 International Atomic Energy Agency, 2002. Modelling the migration and accumulation of  
539 radionuclides in forest ecosystems, Report of the Forest Working Group of the Biosphere  
540 Modelling and Assessment (BIOMASS) Programme, Theme 3. Vienna.

541 International Atomic Energy Agency, 2006. Environmental consequences of the Chernobyl  
542 accident and their remediation: twenty years of experience, Report of the Chernobyl  
543 Forum Expert Group 'Environment'. Radiological Assessment Reports Series. Vienna.

544 International Atomic Energy Agency, 2010. Handbook of parameter values for the prediction  
545 of radionuclide transfer in terrestrial and freshwater environments. Technical Reports  
546 Series. No. 472. Vienna.

547 Japan Aerospace Exploration Agency, 2018. ALOS/ALOS-2 Science Project:  
548 High-Resolution Land Use and Land Cover (HRLULC) map. (Accessed 22 November  
549 2018) at [https://www.eorc.jaxa.jp/ALOS/en/lulc/lulc\\_index.htm](https://www.eorc.jaxa.jp/ALOS/en/lulc/lulc_index.htm).

550 Japan Atomic Energy Agency, 2018. Database for Radioactive Substance Monitoring Data -  
551 Aquatic Organisms in Fresh Water. (Accessed 20 September 2018) at  
552 <http://emdb.jaea.go.jp/emdb/en/>.

553 Japan Fisheries Research and Education Agency, 2017. 平成 28 年度放射性物質影響解明  
554 調査事業報告書 (FY2016 Report of the investigations to understand the effect of  
555 radionuclide) (in Japanese). (Accessed 20 September 2018) at  
556 <http://www.jfa.maff.go.jp/j/housyanou/attach/pdf/kekka-114.pdf>.

557 Japan Meteorological Agency, 2018. Annual average values for each month and each year in

558 Fukushima (Accessed 23 October 2018) at  
559 [https://www.data.jma.go.jp/obd/stats/etrn/view/nml\\_sfc\\_ym.php?prec\\_no=36&block\\_no](https://www.data.jma.go.jp/obd/stats/etrn/view/nml_sfc_ym.php?prec_no=36&block_no)  
560 [=47595](https://www.data.jma.go.jp/obd/stats/etrn/view/nml_sfc_ym.php?prec_no=36&block_no).

561 Kato, H., Onda, Y., Hisadome, K., Loffredo, N., Kawamori, A., 2017. Temporal changes in  
562 radiocesium deposition in various forest stands following the Fukushima Dai-ichi  
563 Nuclear Power Plant accident. *J. Environ. Radioact.* 166(3), 449–457. doi:  
564 10.1016/j.jenvrad.2015.04.016.

565 Kato, H., Onda, Y., Wakahara, T., Kawamori, A., 2018a. Spatial pattern of atmospherically  
566 deposited radiocesium on the forest floor in the early phase of the Fukushima Daiichi  
567 Nuclear Power Plant accident. *Sci. Total Environ.* 615, 187-196. doi:  
568 10.1016/j.scitotenv.2017.09.212.

569 Kato, H., Onda, Y., Saidin, Z.H., Sakashita, W., Hisadome, K., Loffredo, N., 2018b. Six-year  
570 monitoring study of radiocesium transfer in forest environments following the  
571 Fukushima nuclear power plant accident. *J. Environ. Radioact.* In press. doi:  
572 10.1016/j.jenvrad.2018.09.015.

573 Koarashi, J., Atarashi-Andoh, M., Amano, H., Matsunaga, T., 2017. Vertical distributions of  
574 global fallout  $^{137}\text{Cs}$  and  $^{14}\text{C}$  in a Japanese forest soil profile and their implications for the  
575 fate and migration processes of Fukushima-derived  $^{137}\text{Cs}$ . *J. Radioanal. Nucl. Chem.* 311,  
576 473-481. doi: 10.1007/s10967-016-4938-7.

577 Koarashi, J., Atarashi-Andoh, M., 2019. Low  $^{137}\text{Cs}$  retention capability of organic layers in  
578 Japanese forest ecosystems affected by the Fukushima nuclear accident. *J. Radioanal.*  
579 *Nuc. Chem.* 320, 179-191. doi: 10.1007/s10967-019-06435-7.

580 Koarashi, J., Nishimura, S., Atarashi-Andoh, M., Muto, K., Matsunaga, T., A new perspective  
581 on the  $^{137}\text{Cs}$  retention mechanism in surface soils during the early stage after the  
582 Fukushima nuclear accident. *Sci. Rep.* 9, 7034. doi: 10.1038/s41598-019-43499-7.

583 Kochi, K., Mishima, Y., Nagasaka, A., 2010. Lateral input of particulate organic matter from  
584 bank slopes surpasses direct litter fall in the uppermost reaches of a headwater stream in  
585 Hokkaido, Japan. *Limnology*, 11, 77-84. doi: 10.1007/s10201-009-0290-8.

586 Komatsu, M., Kaneko, S., Ohashi, S., Kuroda, K., Sano, T., Ikeda, S., Saito, S., Kiyono, Y.,  
587 Tonosaki, M., Miura, S., Akama, A., Kajimoto, T., Takahashi, M., 2016. Characteristics  
588 of initial deposition and behavior of radiocesium in forest ecosystems of different  
589 locations and species affected by the Fukushima Daiichi Nuclear Power Plant accident. *J.*  
590 *Environ. Radioact.* 161, 2–10. doi: 10.1016/j.jenvrad.2015.09.016.

591 Ministry of Agriculture, Forestry and Fisheries, 2018a. Results of the monitoring on  
592 radioactivity level in fisheries products. (Accessed 18 December 2018) at  
593 <http://www.jfa.maff.go.jp/e/inspection/index.html>.

594 Ministry of Agriculture, Forestry and Fisheries, 2018b. 平成 29 年度 森林内の放射性物質  
595 の分布状況調査結果について (Results of investigations for radionuclide distributions  
596 in forests FY2017) (in Japanese). (Accessed 20 September 2018) at  
597 [http://www.rinya.maff.go.jp/j/kaihatu/jyosen/H29\\_jittaihaaku.html](http://www.rinya.maff.go.jp/j/kaihatu/jyosen/H29_jittaihaaku.html).

598 Ministry of Environment, 2018. 東日本大震災の被災地における放射性物質関連の環境  
599 モニタリング調査: 公共用水域 (Environmental monitoring related to radionuclides in  
600 the area affected by the Great East Japan Earthquake: Public waters) (in Japanese).  
601 (Accessed 20 September 2018) at  
602 [http://www.env.go.jp/jishin/monitoring/results\\_r-pw-h29.html](http://www.env.go.jp/jishin/monitoring/results_r-pw-h29.html).

603 Mukai, H., Tamura, K., Kikuchi, R., Takahashi, Y., Yaita, T., Kogure, T., 2018. Cesium  
604 desorption behavior of weathered biotite in Fukushima considering the actual radioactive  
605 contamination level of soils. *J. Environ. Radioact.* 81–88. 190–191. doi:  
606 10.1016/j.jenvrad.2018.05.006.

607 Murakami, M., Ohte, N., Suzuki, T., Ishii, N., Igarashi, Y., Tanoi, K., 2014. Biological

608 proliferation of cesium-137 through the detrital food chain in a forest ecosystem in Japan.  
609 Sci. Rep. 4, 3599. doi:10.1038/srep03599.

610 Murota, K., Saito, T., Tanaka, S., 2016. Desorption kinetics of cesium from Fukushima soils. J.  
611 Environ. Radioact. 153, 134–140. doi: 10.1016/j.jenvrad.2015.12.013.

612 Nagao, S., Kanamori, M., Ochiai, S., Tomihara, S., Fukushi, K., Yamamoto, M., 2013. Export  
613 of  $^{134}\text{Cs}$  and  $^{137}\text{Cs}$  in the Fukushima river systems at heavy rains by typhoon roke in  
614 september 2011. Biogeosciences 10, 6215-6223.

615 Nakanishi, T., Matsunaga, T., Koarashi, J., Atarashi-Andoh, M., 2014.  $^{137}\text{Cs}$  vertical migration  
616 in a deciduous forest soil following the Fukushima Dai-ichi nuclear power plant accident.  
617 J. Environ. Radioact. 128, 9-14. doi: 10.1016/j.jenvrad.2013.10.019.

618 Nakanishi, T., Sakuma, K., 2018. Trend of  $^{137}\text{Cs}$  concentration in river water in the medium  
619 term and future following the Fukushima nuclear accident. Chemosphere 215, pp.  
620 272-279. doi: 10.1016/j.chemosphere.2018.10.017.

621 Nasvit, O., Klenus, V., Belyaev, V., Volkova, O., Yurchuk, L., Ryabov, O., 2007. Radionuclide  
622 contamination of fish, in: Onishi, Y., Voitsekhovich, O.V., Zheleznyak, M.J. (Eds.),  
623 Chernobyl – what have we learned? The successes and failures to mitigate water  
624 contamination over 20 years. Springer, pp. 66-81.

625 Niizato, T., Abe, H., Mitachi, K., Sasaki, Y., Ishii, Y., Watanabe, T., 2016. Input and output  
626 budgets of radiocesium concerning the forest floor in the mountain forest of Fukushima  
627 released from the TEPCO's Fukushima Dai-ichi nuclear power plant accident. J. Environ.  
628 Radioact. 161, 11-21. doi: 10.1016/j.jenvrad.2016.04.017.

629 Nishina, K., Hayashi, S., 2015. Modeling radionuclide Cs and C dynamics in an artificial  
630 forest ecosystem in Japan -FoRothCs ver1.0-. Frontiers in Environ. Sci. 3, 61. doi:  
631 10.3389/fenvs.2015.00061.

632 Nishina, K., Hashimoto, S., Imamura, N., Ohashi, S., Komatsu, M., Kaneko, S., Hayashi, S.,

633 2018. Calibration of forest  $^{137}\text{Cs}$  cycling model "FoRothCs" via approximate Bayesian  
634 computation based on 6-year observations from plantation forests in Fukushima. *J.*  
635 *Environ. Radioact.* 193-194, 82–90. doi: 10.1016/j.jenvrad.2018.09.002.

636 Nuclear Regulation Authority, 2018. Airborne Monitoring Survey Results. (Accessed 23  
637 October 2018) at <http://radioactivity.nsr.go.jp/en/list/307/list-1.html>.

638 Ochiai, S., Ueda, S., Hasegawa, H., Kakiuchi, H., Akata, N., Ohtsuka, Y., Hisamatsu, S., 2015.  
639 Effects of radiocesium inventory on  $^{137}\text{Cs}$  concentrations in river waters of Fukushima,  
640 Japan, under base-flow conditions. *J. Environ. Radioact.* 144, 86–95. doi:  
641 10.1016/j.jenvrad.2015.03.005.

642 Onishi, Y., Kurikami, H., Yokuda, S.T., 2014. Simulation of sediment and cesium transport in  
643 the Ukedo river and the Ogi dam reservoir during a rainfall event using the TODAM  
644 code. PNNL-23255, Pacific Northwest National Laboratory, Richland, Washington.

645 Rowan, D. J., Chant, L. A., Rasmussen, J. B., 1998. The fate of radiocesium in freshwater  
646 communities - why is biomagnification variable both within and between species? *J.*  
647 *Environ. Radioact.* 40, 15-36.

648 Saito, K., Onda, Y., 2015. Outline of the national mapping projects implemented after the  
649 Fukushima accident. *J. Environ. Radioact.* 139, 240-249. doi:  
650 10.1016/j.jenvrad.2014.10.009.

651 Sakai, M., Gomi, T., Naito, R.S., Negishi, J.N., Sasaki, M., Toda, H., Nunokawa, M., Murase,  
652 K., 2015. Radiocesium leaching from contaminated litter in forest streams. *J. Environ.*  
653 *Radioact.* 144, 15-20. doi: 10.1016/j.jenvrad.2015.03.001.

654 Sakai, M., Gomi, T., Negishi, J.N., Iwamoto, A., Okada, K., 2016a. Different cesium-137  
655 transfers to forest and stream ecosystems. *Environ. Pollut.* 209, 46-52. doi:  
656 10.1016/j.envpol.2015.11.025.

657 Sakai, M., Gomi, T., Negishi, J.N., 2016b. Fallout volume and litter type affect  $^{137}\text{Cs}$

658 concentration difference in litter between forest and stream environments. *J. Environ.*  
659 *Radioact.* 164, 169-173. doi: 10.1016/j.jenvrad.2016.07.030.

660 Sakuma, K., Tsuji, H., Hayashi, S., Funaki, H., Malins, A., Yoshimura, K., Kurikami, H.,  
661 Kitamura, A., Iijima, K., Hosomi, M., Applicability of  $K_d$  for modelling dissolved  $^{137}\text{Cs}$   
662 concentrations in Fukushima river water: Case study of the upstream Ota River. *J.*  
663 *Environ. Radioact.* 184-185, 53-62. doi: 10.1016/j.jenvrad.2018.01.001.

664 Smith, J.T., Konoplev, A., Bulgakov, A.A., Comans, R.N.J., Cross, M.A., Kaminski, S.,  
665 Khristuk, B., Klemt, E., de Koning, A., Kudelsky, A.V., Laptev, G., Madruga, M.J.,  
666 Voitsekhovitch, O., Zibold, G., 2002. AQUASCOPE Technical Deliverable. Simplified  
667 models for predicting  $^{89}\text{Sr}$ ,  $^{90}\text{Sr}$ ,  $^{134}\text{Cs}$ ,  $^{137}\text{Cs}$ ,  $^{131}\text{I}$  in water and fish of rivers, lakes and  
668 reservoirs. CEH Centre for Ecology and Hydrology, Natural Environment Research  
669 Council.

670 Spezzano, P., Hilton, J., Lishman, J.P., Carrick, T.R., 1993. The variability of Chernobyl Cs  
671 retention in the water column of lakes in the English Lake District, two years and four  
672 years after deposition. *J. Environ. Radioact.* 19, 213-232. doi:  
673 10.1016/0265-931X(93)90004-Q.

674 Sundbom, M., Meili, M., Andersson, E., Östlund, M., Broberg, A., 2003. Long-term dynamics  
675 of Chernobyl  $^{137}\text{Cs}$  in freshwater fish: quantifying the effect of body size and trophic  
676 level. *J. Applied Ecology.* 40, 228-240.

677 Tagami, K., Uchida, S., 2016. Consideration on the long ecological half-life component of  
678  $^{137}\text{Cs}$  in demersal fish based on field observation results obtained after the Fukushima  
679 accident. *Environ. Sci. Technol.*, 50(4), 1804-1811. doi: 10.1021/acs.est.5b04952.

680 Takada, M., Yamada, T., Takahara, T., Okuda, T., 2016. Spatial variation in the  $^{137}\text{Cs}$  inventory  
681 in soils in a mixed deciduous forest in Fukushima, Japan. *J. Environ. Radioact.* 161,  
682 35-41. doi: 10.1016/j.jenvrad.2016.04.033.

683 Thiry, Y., Albrecht, A., Tanaka, T., 2018. Development and assessment of a simple ecological  
684 model (TRIPS) for forests contaminated by radiocesium fallout. *J. Environ. Radioact.*  
685 190-191, 149-159. doi: 10.1016/j.jenvrad.2018.05.009.

686 Tonin, A.M., Gonçalves, J.F., Bambi, P., Couceiro, S.R.M., Feitoza, L.A.M., Fontana, L.E.,  
687 Hamada, N., Hepp, L.U., Lezan-Kowalczyk, V.G., Leite, G.F.M., Lemes-Silva, A.L.,  
688 Lisboa, L.K., Loureiro, R.C., Martins, R.T., Medeiros, A.O., Morais, P.B., Moretto, Y.,  
689 Oliveria, P.C.A., Pereira, E.B., Ferreira, L.P., Pérez, J., Petrucio, M.M., Reis, D.F.,  
690 Rezende, R.S., Roque, N., Santos, L.E.P., Siegloch, A.E., Tonello, G., Boyero, L., 2017.  
691 Plant litter dynamics in the foreststream interface: precipitation is a major control across  
692 tropical biomes. *Sci. Rep.* 7, 10799. doi: 10.1038/s41598-017-10576-8.

693 Tsuji, H., Nishikiori, T., Yasutaka, T., Watanabe, M., Ito, S., Hayashi, S., 2016. Behavior of  
694 dissolved radiocesium in river water in a forested watershed in Fukushima prefecture. *J.*  
695 *Geophys. Res.: Biogeosciences* 121, 2588–2599. doi: 10.1002/2016JG003428.

696 Tuovinen, T. S., Saengkul, C., Ylipieti, J., Solatie, D., Juutilainen, J., 2012. Transfer of <sup>137</sup>Cs  
697 from water to fish is not linear in two northern lakes. *Hydrobiologia.* 700 (1), 131-139.  
698 doi: 10.1007/s10750-012-1224-8.

699 Ueda, S., Hasegawa, H., Kakiuchi, H., Akata, N., Ohtsuka, Y., Hisamatsu, S., 2013. Fluvial  
700 discharges of radiocaesium from watersheds contaminated by the Fukushima Dai-ichi  
701 Nuclear Power Plant accident, Japan. *J. Environ. Radioact.* 118, 96-104. doi:  
702 10.1016/j.jenvrad.2012.11.009.

703 Unoki, S., 2010. 流系の科学 (Science in flow water systems) (in Japanese). first ed.  
704 Tsukiji-shokan, Tokyo.

705 Wada, T., Tomiya, A., Enomoto, M., Sato, T., Morishita, D., Izumi, S., Niizeki, K., Suzuki, S.,  
706 Morita, T., Kawata, G., 2016a. Radiological impact of the nuclear power plant accident  
707 on freshwater fish in Fukushima: An overview of monitoring results. *J. Environ.*

708 Radioact. 151, 144-155. doi: 10.1016/j.jenvrad.2015.09.017.

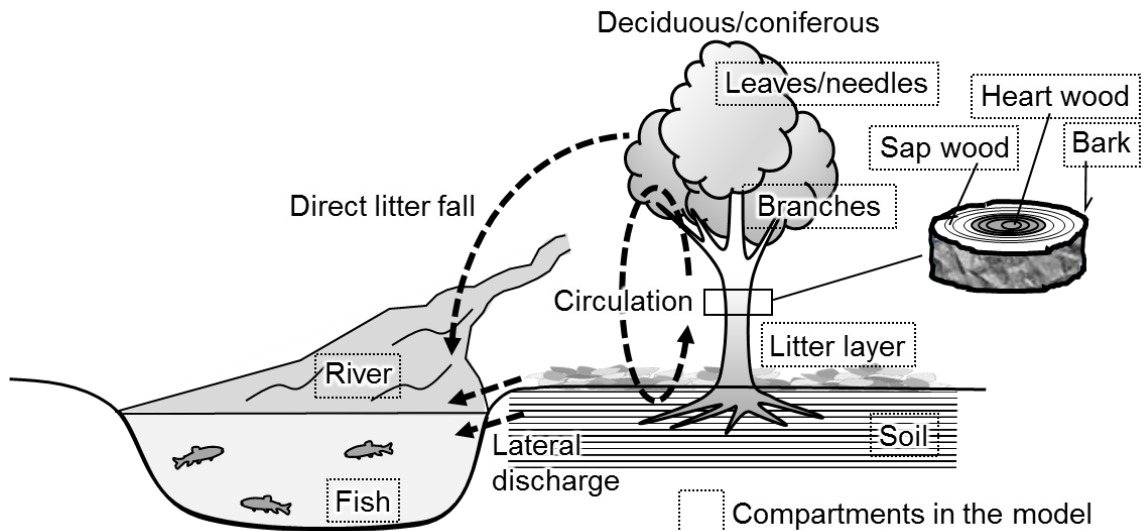
709 Wada, T., Fujita, T., Nemoto, Y., Shimamura, S., Mizuno, T., Sohtome, T., Kamiyama, K.,  
710 Narita, K., Watanabe, M., Hatta, N., Ogata, Y., Morita, T., Igarashi, S., 2016b. Effects of  
711 the nuclear disaster on marine products in Fukushima: An update after five years. J.  
712 Environ. Radioact. 164, 312-324. doi: 10.1016/j.jenvrad.2016.06.028.

713 Wada, T., Konoplev, A., Wakiyama, Y., Watanabe, K., Furuta, Y., Morishita, D., Kawata, G.,  
714 Nanba, K., 2019. Strong contrast of cesium radioactivity between marine and freshwater  
715 fish in Fukushima. J. Environ. Radioact. 204, 132-142. doi:  
716 10.1016/j.jenvrad.2019.04.006.

717 Yamaguchi, M., Kitamura, A., Oda, Y., Onishi, Y., 2014. Predicting the long-term <sup>137</sup>Cs  
718 distribution in Fukushima after the Fukushima Dai-ichi nuclear power plant accident: a  
719 parameter sensitivity analysis. J. Environ. Radioact. 135, 135-146. doi:  
720 10.1016/j.jenvrad.2014.04.011.

721 Yamashiki, Y., Onda, Y., Smith, H.G., Blake, W.H., Wakahara, T., Igarashi, Y., Matsuura, Y.,  
722 Yoshimura, K., 2014. Initial flux of sediment-associated radiocesium to the ocean from  
723 the largest river impacted by Fukushima Daiichi Nuclear Power Plant. Sci. Rep. 4, 3714.  
724 doi: 10.1038/srep03714.

725 Yoshimura, K., Onda, Y., Sakaguchi, A., Yamamoto, M., Matsuura, Y., 2015. An extensive  
726 study of the concentrations of particulate/dissolved radiocaesium derived from the  
727 Fukushima Dai-ichi Nuclear Power Plant accident in various river systems and their  
728 relationship with catchment inventory. J. Environ. Radioact. 139, 370-378. doi:  
729 10.1016/j.jenvrad.2014.08.021.



730

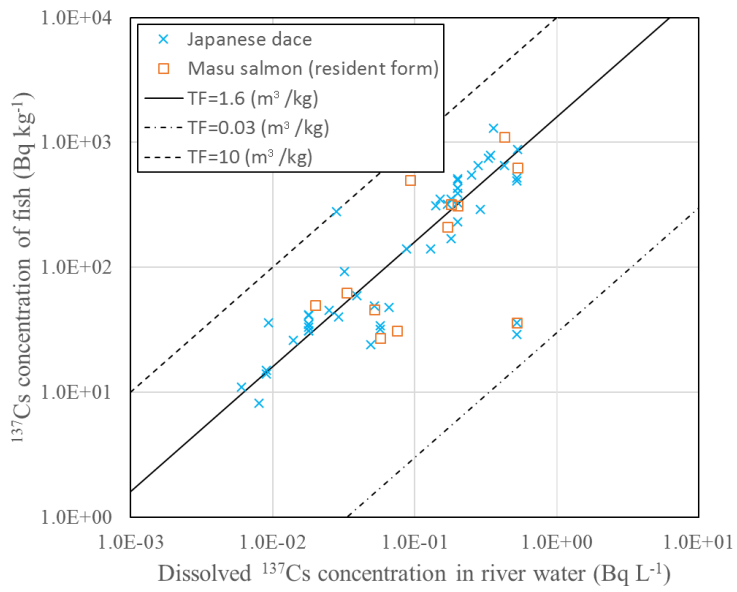
731 Fig. 1 Schematic of the compartments in the model.

comp., from	to	<i>j</i> =1 Leaves/ needles	2 Branches	3 Bark	4 Sap wood	5 Heart wood	6 Litter layer	7 Soil	8-14 <i>Coniferous forest</i>	15 River	16 Down- stream	Fish						
Atmo- sphere		intercept.	intercept.	intercept.			intercept.		intercept.	direct fallout								
<i>Deciduous forest</i>		<div style="border: 1px solid black; width: 100%; height: 100%;"></div>																
<i>i</i> =1 Leaves/ needles	-								translo- cation	weather- ing			litter fall, weathering			direct litter fall		
2 Branches	translo- cation								-	weather- ing	translo- cation	translo- cation	litter fall, weathering					
3 Bark										-	translo- cation		weathering					
4 Sap wood									translo- cation	translo- cation	-	translo- cation						
5 Heart wood											translo- cation	-						
6 Litter layer											root uptake		-	decomp., infiltrate.		lateral inflow		
7 Soil				root uptake			-		lateral inflow									
<i>Coniferous forest</i>		<div style="border: 1px solid black; width: 100%; height: 100%;"></div>																
8-14 ( <i>comparte- nts same as deciduous forest</i> )													same as <i>deciduous forest</i>		Direct litter fall, lateral inflow			
15 River		<div style="border: 1px solid black; width: 100%; height: 100%;"></div>								-	river flow	uptake						

732 Fig. 2 Interaction matrix of the compartments. Processes listed in each light shaded box

733 represent the transfer processes modelled from compartment *i* to compartment *j*. Blank

734 interactions means there no transfer between those compartments.



735

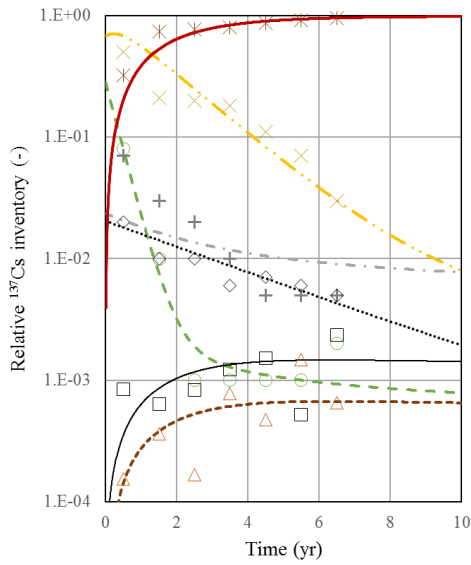
736 Fig. 3 Relationship between fish and dissolved river water <sup>137</sup>Cs concentrations.

737 Measurements by [Ministry of Environment \(2018\)](#).

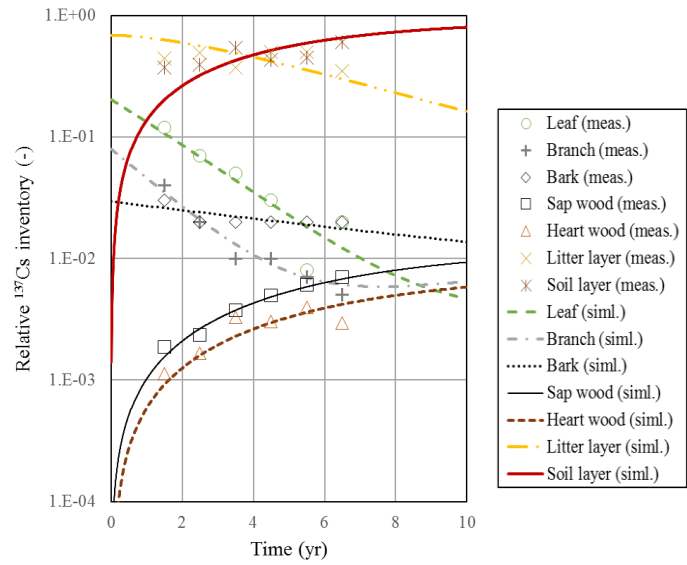
738

739

740 (a)

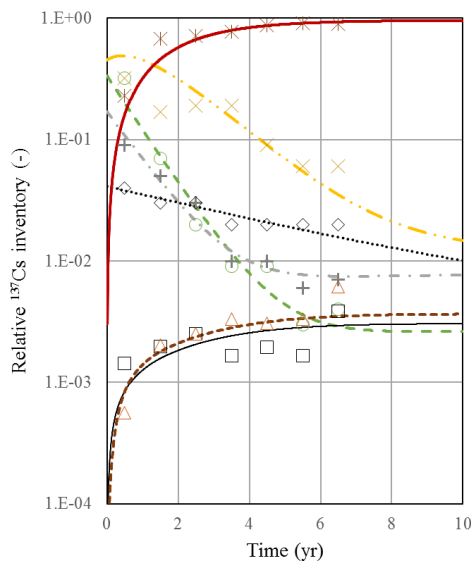


(b)

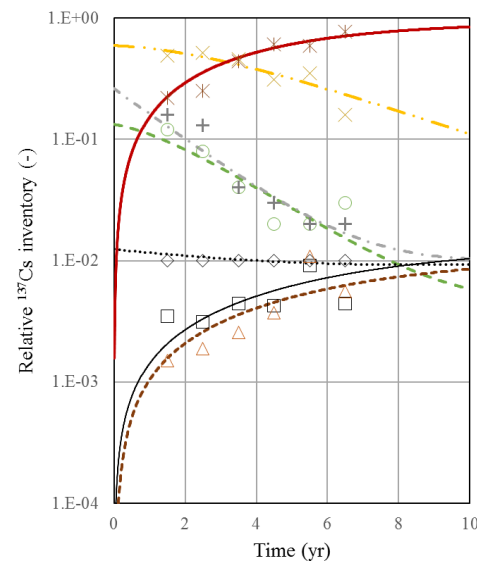


741

742 (c)



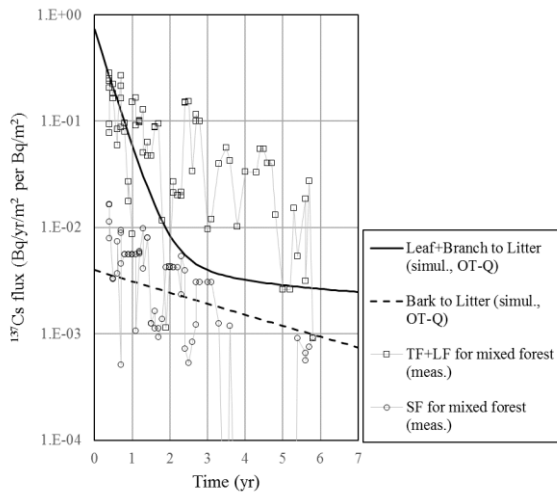
(d)



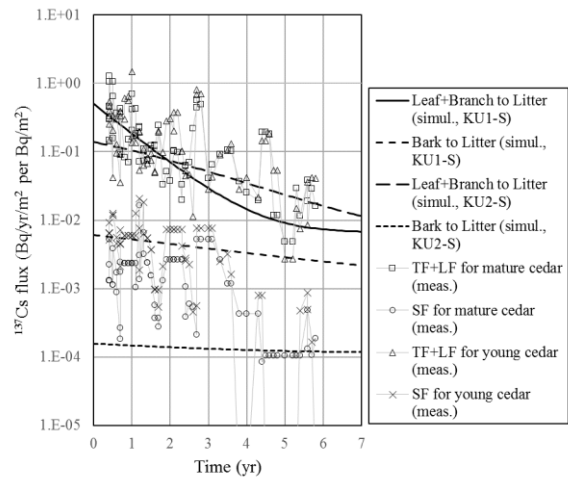
743

744 Fig. 4 Relative  $^{137}\text{Cs}$  inventory of forest compartments after inverse fitting for transfers  
 745 parameters and initial state. Graphs show measurements from [Ministry of Agriculture,](#)  
 746 [Forestry and Fisheries \(2018\)](#) (symbols) and compartment model results (lines). (a) Konara  
 747 oak forest in Otama (OT-Q) – leaf, litter and soil compartment  $w_i=5$ . (b) Hinoki forest in  
 748 Kawauchi (KU1-H), (c) sugi cedar forest in Kawauchi (KU1-S), and (d) second sugi cedar  
 749 forest in Kawauchi (KU2-S) – all  $w_i=1$ .

750 (a)



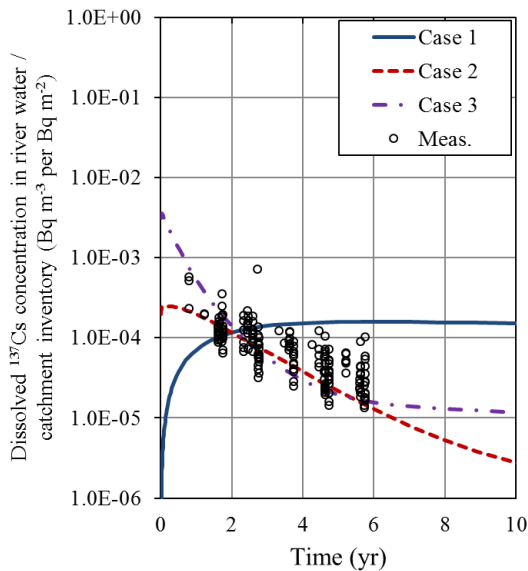
(b)



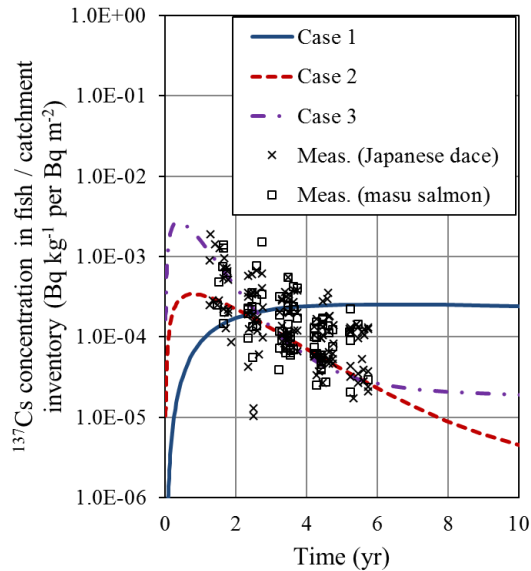
751

752 Fig.5 Comparison of  $^{137}\text{Cs}$  fluxes from the canopy to the forest floor between the  
 753 parametrized simulations and independent measurements by [Kato et al. \(2018b\)](#): (a) simulated  
 754 konara oak forest at Otama compared with the Kawamata mixed forest, (b) simulated sugi  
 755 cedar compared with Kawamata cedar forests.

756 (a)



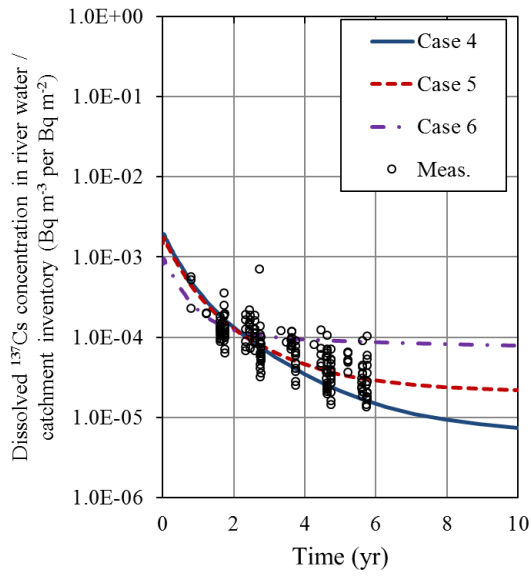
(b)



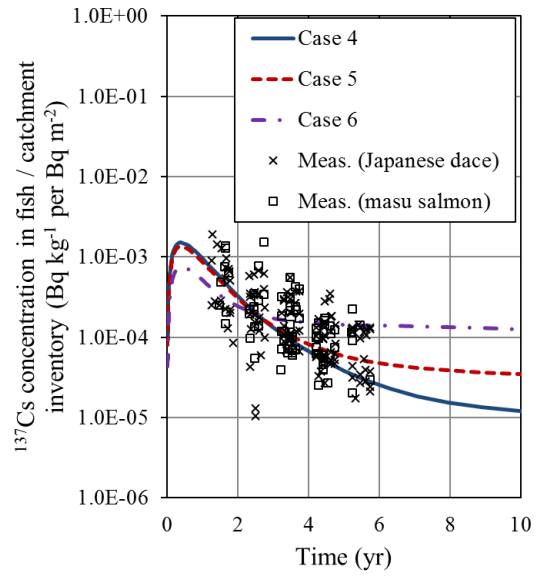
757

758 Fig. 6 Simulation results of Case 1 to 3 compared with measurements by the [Ministry of](#)  
 759 [Environment \(2018\)](#) and the [Japan Fisheries Research and Education Agency \(2017\)](#):  $^{137}\text{Cs}$   
 760 concentrations in (a) river water and (b) freshwater fish.

761 (a)



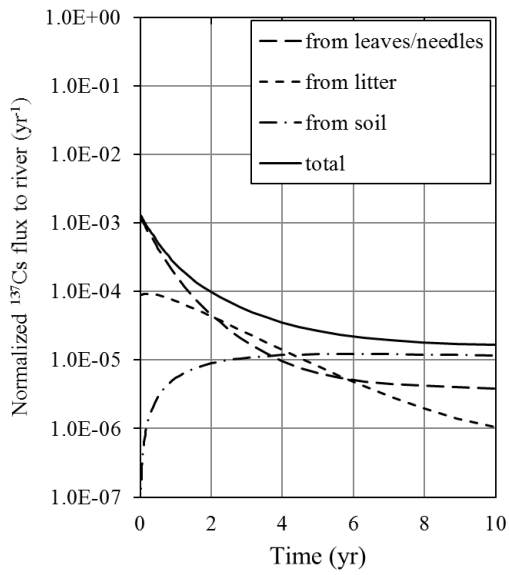
(b)



762

763 Fig. 7 Simulation results of Case 4 to 6 compared with measurements:  $^{137}\text{Cs}$  concentrations in

764 (a) river water and (b) freshwater fish.



765

766 Fig. 8 Normalized relative fluxes of dissolved  $^{137}\text{Cs}$  input into river water in Case 5.

767 Table 1 Concentrations of <sup>137</sup>Cs in muscle of major freshwater fish species in Fukushima  
 768 Prefecture.

Species	Concentration of <sup>137</sup> Cs (Bq kg <sup>-1</sup> )	
	Outside the evacuation zone (April 2018 to March 2019) MAFF (2018a)	Inside the evacuation zone (caught in 2016) Fukushima Prefecture (2018b)
Ayu ( <i>Plecoglossus altivelis</i> )	N.D. - 53.5	Up to 2000
Masu salmon ( <i>Oncorhynchus masou</i> ) (resident form)	N.D. - 126	Up to 20000
White-spotted char ( <i>Salvelinus leucomaenis</i> )	N.D. - 195	n.a.
Japanese dace ( <i>Tribolodon hakonensis</i> )	N.D. - 50.4	n.a.
Japanese eel ( <i>Anguilla japonica</i> )	N.D. - 22.8	n.a.
Common carp ( <i>Cyprinus carpio</i> )	N.D. - 23.9	n.a.

769 N.D.: not detected. The detection limit is about 5 to 10 Bq kg<sup>-1</sup>. n.a.: no applicable measurements.

770 Table 2 Simulation cases for parameter exploration.

		Transfer rates (yr <sup>-1</sup> ) (percentage of the total discharge flux from forests at two years)		
		From leaves/needles to river	From litter layer to river	From soil to river
Case 1	Single process	0	0	1.4E-4 (100%)
Case 2	Single process	0	2.7E-4 (100%)	0
Case 3	Single process	9.3E-3 (100%)	0	0
Case 4	Multiple processes	4.7E-3 (50%)	1.4E-4 (50%)	0 (0%)
Case 5	Multiple processes	4.2E-3 (45%)	1.2E-4 (45%)	1.4E-5 (10%)
Case 6	Multiple processes	2.3E-3 (25%)	6.8E-4 (25%)	7.0E-5 (50%)

771 Table 3 Initial fallout interception ratios estimated by inverse fitting analysis.

	Initial interception ratio			
	Deciduous forest	Coniferous forest		
	Konara oak forest in Otama (OT-Q)	Hinoki cypress forest in Kawauchi (KU1-H)	Sugi cedar forest in Kawauchi (KU1-S)	Sugi cedar forest in Kawauchi (KU2-S)
Simulation results				
Leaves/needles	0.28	0.20	0.34	0.13
Branches	0.02	0.08	0.17	0.26
Bark	0.02	0.03	0.04	0.01
Tree total	0.32	0.31	0.55	0.41
Measurement (Kato et al., 2017)	0.23 for the mixed forest	0.69 for the mature cedar forest and 0.70 for the young cedar forest		

772

773

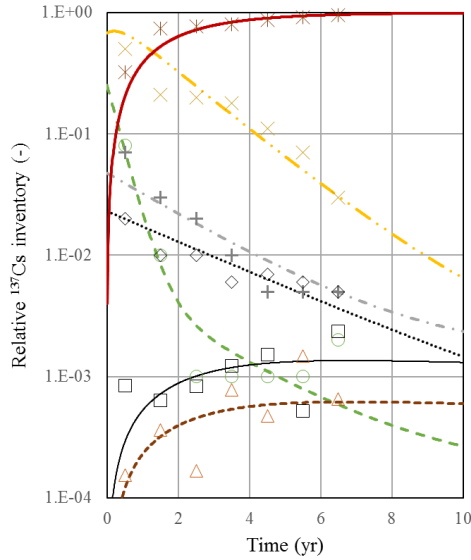
774 Table 4 Transfer rates between forest compartments estimated by inverse fitting analysis.

Transfer process	Transfer rates (yr <sup>-1</sup> )			
	Konara oak forest in Otama (OT-Q)	Hinoki cypress forest in Kawauchi (KU1-H)	Sugi cedar forest in Kawauchi (KU1-S)	Sugi cedar forest in Kawauchi (KU2-S)
Leaves/needles to branches	3.8 x 10 <sup>-4</sup>	8.0 x 10 <sup>-3</sup>	2.6 x 10 <sup>-3</sup>	5.3 x 10 <sup>-3</sup>
Leaves/needles to bark	5.4 x 10 <sup>-5</sup>	2.3 x 10 <sup>-4</sup>	2.1 x 10 <sup>-3</sup>	1.7 x 10 <sup>-3</sup>
Leaves/needles to litter layer	2.6	0.52	1.3	0.69
Branches to leaves	0.26	0.29	0.44	0.30
Branches to bark	1.2 x 10 <sup>-5</sup>	3.3 x 10 <sup>-4</sup>	1.1 x 10 <sup>-4</sup>	2.4 x 10 <sup>-4</sup>
Branches to sap wood	7.2 x 10 <sup>-4</sup>	4.8 x 10 <sup>-4</sup>	1.8 x 10 <sup>-2</sup>	2.5 x 10 <sup>-3</sup>
Branches to heart wood	1.8 x 10 <sup>-3</sup>	1.4 x 10 <sup>-3</sup>	6.7 x 10 <sup>-3</sup>	2.3 x 10 <sup>-3</sup>
Branches to litter layer	1.7 x 10 <sup>-2</sup>	0.29	0.45	0.18
Bark to sap wood	4.9 x 10 <sup>-2</sup>	4.2 x 10 <sup>-2</sup>	1.7 x 10 <sup>-2</sup>	7.8 x 10 <sup>-2</sup>
Bark to litter layer	0.20	4.2 x 10 <sup>-2</sup>	0.15	1.3 x 10 <sup>-2</sup>
Sap wood to branches	1.4	0.44	2.3	0.45
Sap wood to bark	3.6 x 10 <sup>-2</sup>	2.3 x 10 <sup>-2</sup>	0.16	8.8 x 10 <sup>-2</sup>
Sap wood to heart wood	6.0	6.8	4.8	4.2
Heart wood to sap wood	13	11	4.0	5.0
Litter layer to sap wood	1.1 x 10 <sup>-4</sup>	2.3 x 10 <sup>-4</sup>	2.7 x 10 <sup>-5</sup>	7.2 x 10 <sup>-4</sup>
Litter layer to soil	0.59	0.20	0.67	0.26
Soil to sap wood	1.9 x 10 <sup>-3</sup>	5.7 x 10 <sup>-3</sup>	7.4 x 10 <sup>-3</sup>	6.9 x 10 <sup>-3</sup>

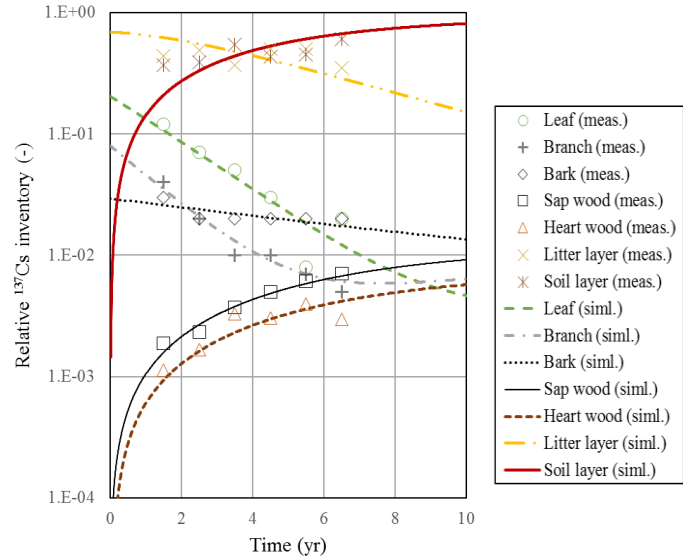
775

776 Supplementary Information to Numerical study of transport pathways of  $^{137}\text{Cs}$  from forests to  
 777 freshwater fish living in mountain streams in Fukushima, Japan

778 (a)

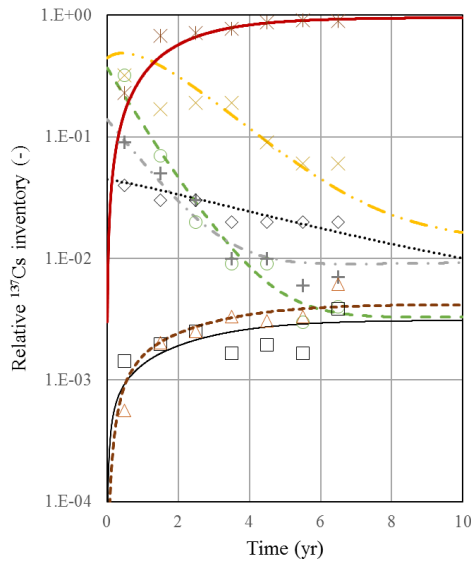


(b)

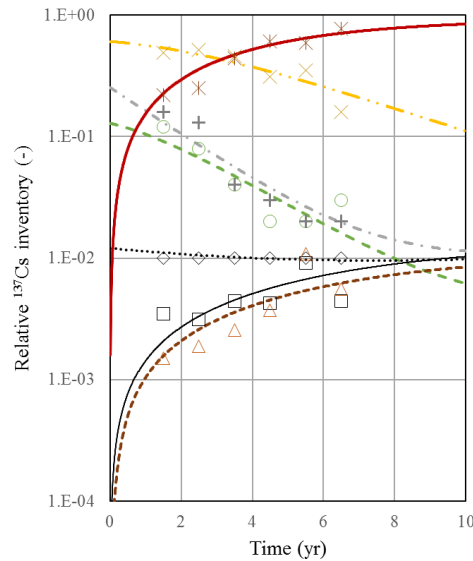


779

780 (c)



(d)



781

782 Fig. S1 As per Fig. 4 of main text, but showing compartment results obtained using different  
 783 weights  $w_i$  in the parameter fitting process. (a) Konara oak forest in Otama (OT-Q) – all  
 784 compartments  $w_i=1$ . (b) Hinoki forest in Kawauchi (KU1-H), (c) sugi cedar forest in  
 785 Kawauchi (KU1-S) and (d) second sugi cedar forest in Kawauchi (KU2-S) – needle, litter and  
 786 soil compartments  $w_i=5$ .